ChemComm

RSC Publishing

COMMUNICATION

View Article Online
View Journal | View Issue

Selective surface functionalization at regions of high local curvature in graphene†

Cite this: *Chem. Commun.*, 2013, **49**, 677

Received 17th September 2012,
Accepted 26th November 2012

DOI: 10.1039/c2cc36747e

www.rsc.org/chemcomm

Qingzhi Wu,[ab] Yaping Wu,[b] Yufeng Hao,[b] Jianxin Geng,[c] Matthew Charlton,[b] Shanshan Chen,[b] Yujie Ren,[b] Hengxing Ji,[b] Huifeng Li,[b] Danil W. Boukhvalov,[d] Richard D. Piner,[b] Christopher W. Bielawski*[ce] and Rodney S. Ruoff*[b]

Monolayer graphene was deposited on a Si wafer substrate decorated with SiO_2 nanoparticles (NPs) and then exposed to aryl radicals that were generated *in situ* from their diazonium precursors. Using micro-Raman mapping, the aryl radicals were found to selectively react with the regions of graphene that covered the NPs. The enhanced chemical reactivity was attributed to the increased strain energy induced by the local mechanical deformation of the graphene.

On account of its exceptionally high carrier mobility, thermal conductivity, and mechanical properties, graphene has attracted considerable attention for use in nanoelectronics, supercapacitors and thermal management applications, among others.[1–4] However, the zero bandgap of graphene is a drawback for applications that require controlled conductivities, such as logic gates. Thus, there is interest in the synthesis of quasi one-dimensional graphene nanoribbons, which confine the carriers to specified regions with defined band gaps.[5–8] While chemical doping provides a means to achieve such goals, the doping process introduces defects in a random fashion.[9–13] Indeed, the selective spatial functionalization of graphene remains an important challenge for the field.

It is generally accepted that the carbon atoms located within the plane of graphene are relatively chemically inert due to conjugation, while those located at the edges or at defects are more reactive.[14,15] However, according to 'π-orbital axis vector' (POAV) theory, the carbon atoms that reside on highly curved surfaces should exhibit increased chemical potential due to diminished electronic delocalization.[16–18] They should also display higher strain energies such that increased reactivity may be expected[19,20] and even described using the strain coordinates.[21,22] Indeed, a DFT simulation of the chemical reactivity of corrugated graphene predicted an enhancement if the ratio of the height of the corrugation (ripple) to its radius was larger than 0.07.[23] We envisioned that selectively deforming graphene would render the carbon atoms in the regions of high curvature chemically reactive.[24] To test this hypothesis, graphene was 'suspended' on SiO_2 NPs to introduce local curvature and then exposed to aryl radicals to determine if such curved surfaces were more reactive than the planar regions.

As illustrated in Scheme 1, CVD-grown graphene was transferred to a Si substrate having a 280 nm thick SiO_2 layer and then treated with 4-nitrophenyl diazonium tetrafluoroborate (**1**), which is known to decompose into aryl radicals. Fig. 1a and b show the Raman spectra of graphene on the Si substrate before and after treatment with the diazonium salt. The characteristic signals at *ca.* 1580 and 2670 cm^{-1} were assigned to the G band and 2D bands which derive from the in-plane optical vibration and second-order zone boundary phonons, respectively. The signal at *ca.* 1350 cm^{-1}, which was attributed to the D band derived from first-order zone boundary phonons, was absent in the Raman spectra recorded for the virgin graphene material but was clearly observed after treatment. The presence of the D band in the Raman spectra of the

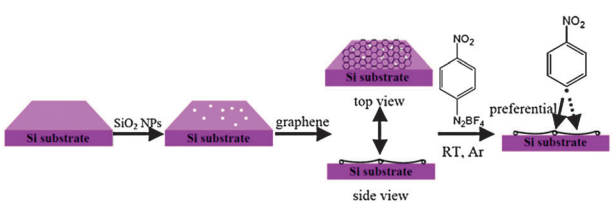

Scheme 1 Transferring graphene onto substrates decorated with SiO_2 NPs facilitated the selective functionalization with aryl radicals in regions of high local curvature.

[a] *State Key Laboratory of Advanced Technology for Materials Synthesis and Processing, and Biomedical Materials and Engineering Center, Wuhan University of Technology, Wuhan 430070, China*
[b] *Department of Mechanical Engineering and the Materials Science and Engineering Program, The University of Texas at Austin, 1 University Station C2200, Austin, TX 78712, USA. E-mail: r.ruoff@mail.utexas.edu*
[c] *Department of Chemistry and Biochemistry, The University of Texas at Austin, 1 University Station A1590, Austin, TX 78712, USA. E-mail: bielawski@cm.utexas.edu*
[d] *School of Computational Sciences, Korea Institute for Advanced Study, Seoul 130-722, Korea*
[e] *World Class University (WCU) Program of Chemical Convergence for Energy & Environment (C_2E_2), School of Chemical and Biological Engineering, Seoul National University, Seoul 151-742, Korea*

† Electronic supplementary information (ESI) available: Additional experimental details, DFT calculations, and Raman spectra. See DOI: 10.1039/c2cc36747e

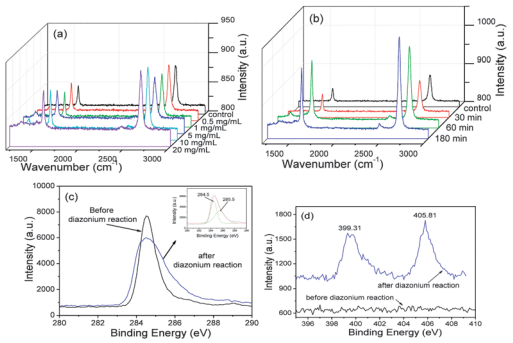

Fig. 1 (a) Raman spectra of graphene before and after chemical treatment using various concentrations of **1**. (b) Raman spectra of graphene before and after treatment for different reaction times. (c) C1s XPS spectra of the graphene before and after treatment (10 mg mL^{-1} of **1** in acetonitrile, 180 min). Inset shows the peak fitting of the C1s spectrum after treatment. (d) N1s XPS spectra of the graphene before and after treatment (10 mg mL^{-1} of **1** in acetonitrile, 180 min).

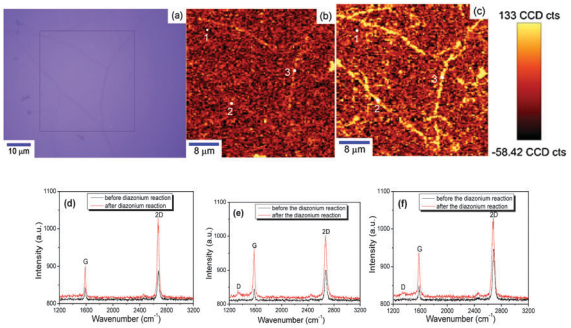

Fig. 2 (a) Optical image of graphene on a Si substrate. Panels (b) and (c) are 2-D Raman maps of the D band region (1300–1400 cm^{-1}) of graphene before and after chemical treatment (10 mg mL^{-1} of **1** in acetonitrile, 60 min). (d)–(f) Raman spectra of graphene before and after chemical treatment, corresponding to points marked with 1, 2, and 3 in (b) and (c), respectively.

graphene exposed to **1** has been previously shown to be due to the covalent attachment of a nitrophenyl group.[11,12,25,26] The intensity of the D band was found to increase over time and in the presence of higher concentrations of the diazonium salt, a result consistent with the transformation of sp^2 to sp^3 bonding of some of the graphene's carbon atoms.[13,25–27] It is noteworthy that the signal intensity in the region between the D band and G band also significantly increased after treatment with **1**, providing further evidence for the change in hybridization.[11,27]

The covalent bonding of nitrobenzene with graphene was further assessed with XPS and the key results are summarized in Fig. 1c and d. The C1s signal observed at *ca.* 284.5 eV broadened and decreased in intensity after exposure to **1**, and was successfully fit with two Gaussian curves with maxima at *ca.* 284.5 and 285.5 eV (Fig. 1c inset). The signal observed at *ca.* 285.5 eV was attributed to the C–N bond of the nitrobenzene group, while the decrease in the intensity of the peak at 284.5 eV was attributed to the decreased number of sp^2 carbons in the lattice due to the change in hybridization.[28–30] The signals observed at *ca.* 399.3 and 405.8 eV (Fig. 1d) were assigned to the nitrophenyl groups;[28–30] no significant signals from B or F were detected (data not shown).

Next, the spatial distribution of the nitrophenyl groups was assessed using 2-D micro-Raman mapping in the D band region (1300–1400 cm^{-1}). The optical image of monolayer graphene on a Si substrate is shown in Fig. 2a. Several wrinkles were observed and are believed to form on account of the thermal expansion coefficients of graphene *vs.* Cu foil.[30] The Raman map marked with the frame in Fig. 2a generally showed a low signal intensity except at some wrinkles (Fig. 2b), demonstrating that the CVD-grown graphene was of high quality and that the D band defects were preferentially formed at these high curvature sites. Fig. 2d–f show three typical Raman spectra at the planar or wrinkled sites of graphene before and after chemical treatment. At the planar site (point 1), no obvious D band was detected (Fig. 2d). However, the intensity of the D band at the wrinkled sites (points 2 and 3) was significantly increased (*i.e.*, a measured I_D/I_G ratio of *ca.* 0.86 and 0.88) after treatment with **1**. The increase of the I_D/I_G ratio along with the wrinkles after treatment was also observed in the Raman map of the I_D/I_G ratio (Fig. S1, ESI†). Collectively, these results suggested to us that the reactivity of the carbon atoms along the wrinkles of graphene was higher than for the carbon atoms in the planar regions.

To further evaluate the curvature-induced enhancement of chemical reactivity of graphene, SiO_2 NPs with an average diameter of *ca.* 50 nm were deposited on the surface of a Si substrate before the graphene was transferred. As shown in Fig. 3, SEM revealed that the graphene featured wrinkles with different degrees of curvature; aggregates of the SiO_2 NPs were also observed (as white dots). The variation in size of the wrinkles was presumed to be due to the propensity of the NPs to form clusters of various sizes. As shown in Fig. 4a, the Raman map of a SiO_2 NP perturbed graphene sheet exhibited an overall low D band intensity before treatment with the diazonium salt although the influence of the SiO_2 NPs was apparent (Fig. 4b). After treatment, a significant enhancement of the D band intensity was observed, particularly in the regions along the wrinkles. Fig. 4d and f show the Raman spectra of the points marked in Fig. 4b and c before and after exposure to the diazonium salt, respectively. At point 1, no significant increase of the D band intensity was observed after treatment, while a significant increase of the D band intensity was observed at points 2 and 3 (corresponding to I_D/I_G ratios of *ca.* 0.85 and 0.86, respectively), indicating that the formation of more 'defects' at these curved

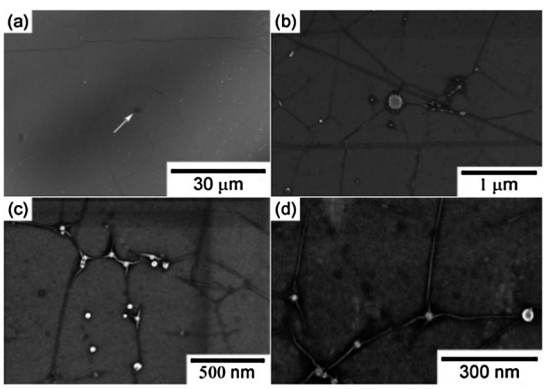

Fig. 3 SEM images of graphene on a Si substrate decorated with SiO_2 nanoparticles. Frames (b)–(d) are higher magnification images of the area marked with the white arrow in (a). Numerous wrinkles induced by the SiO_2 nanoparticles are visible. The shadow marked with the white arrow in (a) was attributed to the extensive irradiation by the electron beam during imaging.

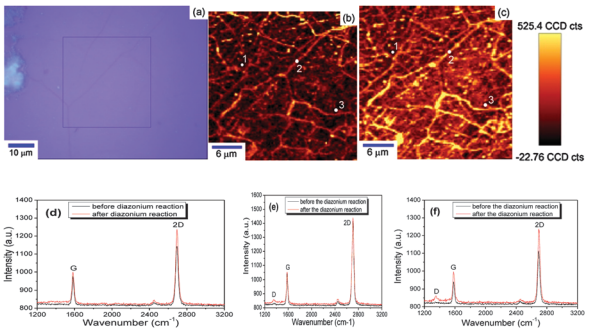

Fig. 4 (a) Optical image of graphene on a Si substrate decorated with SiO_2 NPs. Panels (b) and (c) are the 2-D Raman maps of the D band intensities of graphene before and after chemical treatment (10 mg mL^{-1} **1** in acetonitrile, 60 min). (d)–(f) Typical Raman spectra of graphene before and after treatment, corresponding to the points marked with 1, 2, and 3 in (b) and (c), respectively.

sites was due to the covalent attachment of nitrobenzene. In support of this assessment, Raman mapping of the I_D/I_G ratio showed an increase of the I_D/I_G ratio along the wrinkles after treatment with the diazonium salt (Fig. S2, ESI†).

It is known that carbon atoms at the edges and defects of graphene are more reactive than those in the basal plane.[14,15] However, as we have previously outlined[19,20] and showed above, the carbon atoms in highly curved regions are also reactive. Moreover, theoretical predictions and experimental observations have demonstrated that the electronic properties of graphene may change through the application of mechanical strain.[31–35] Building on these results, the binding energy of a nitrophenyl group to flat and rippled graphene surfaces was calculated using DFT; in parallel, the pyramidalization angles of the ripples were measured *via* POAV theory. The calculations demonstrated that increasing the curvature of the ripples resulted in increased pyramidalization surface reactivity, when the corrugation height to radius ratio was greater than 0.15. Although the mechanism of the aryl radical addition remains under investigation,[36] it appears from our work that the reaction may be guided through the development of local mechanical deformation and other intimately coupled phenomena, including changes in the density of states and electronic chemical potential.

In summary, transferring graphene onto a Si wafer substrate decorated with SiO_2 NPs induced local regions of mechanical strain and increased the chemical reactivity of at least some of the carbon atoms at these sites. In particular, *in situ* generated aryl radicals were found to couple to the graphene regions with a higher degrees of local curvature. It is suggested that future studies use substrates that introduce deformation in well defined areas (*e.g.*, patterned substrates with high aspect features) to not only enable the chemical patterning of graphene but also to enhance its chemical reactivity and potentially electronic properties in a selective manner.

We appreciate advice from K. Ausman. We acknowledge support from the NSF (DMR-0907324), the CSC, the National Natural Science Foundation of China (Grant No. 30800256), and the Program for Changjiang Scholars and Innovative Research Team (IRT1169) at the Wuhan University of Technology. CWB acknowledges the Welch Foundation (F-1621), the ARO (W911NF-07-1-0409), and the WCU program (R31-10013) as administered through the NRF of Korea and funded by the Ministry of Education, Science, and Technology. DWB acknowledges computational support from the CAC of KIAS.

Notes and references

1 A. K. Geim and K. S. Novoselov, *Nat. Mater.*, 2007, **6**, 183.
2 Y. W. Zhu, S. Murali, W. W. Cai, X. S. Li, J. W. Suk, J. R. Potts and R. S. Ruoff, *Adv. Mater.*, 2010, **22**, 3906.
3 D. R. Dreyer, R. S. Ruoff and C. W. Bielawski, *Angew. Chem., Int. Ed.*, 2010, **49**, 9336.
4 J. R. Potts, D. R. Dreyer, C. W. Bielawski and R. S. Ruoff, *Polymer*, 2011, **52**, 5.
5 J. M. Cai, P. Ruffieux, R. Jaafar, M. Bieri, T. Braun, S. Blankenburg, M. Muoth, A. P. Seitsonen, M. Saleh, K. Müllen and R. Fasel, *Nature*, 2010, **466**, 470.
6 K. A. Ritter and J. W. Lyding, *Nat. Mater.*, 2009, **8**, 235.
7 L. Y. Jiao, L. Zhang, X. R. Wang, G. Diankov and H. J. Dai, *Nature*, 2009, **458**, 877.
8 X. T. Jia, M. Hofmann, V. Meunier, B. G. Sumpter, J. Campos-Delgado, J. M. Romo-Herrera, H. Son, Y. P. Hsieh, A. Reina, J. Kong, M. Terrones and M. S. Dresselhaus, *Science*, 2009, **323**, 1701.
9 X. Y. Fan, R. Nouchi, L. C. Yin and K. Tanigaki, *Nanotechnology*, 2010, **21**, 475208.
10 H. T. Liu, S. M. Ryu, Z. Y. Chen, M. L. Steigerwald, C. Nuckolls and L. E. Brus, *J. Am. Chem. Soc.*, 2009, **131**, 17099.
11 P. Huang, H. R. Zhu, L. Jing, Y. L. Zhao and X. Y. Gao, *ACS Nano*, 2011, **5**, 7945.
12 H. Zhang, E. Bekyarova, J. W. Huang, Z. Zhao, W. Z. Bao, F. L. Wang, R. C. Haddon and C. N. Lau, *Nano Lett.*, 2011, **11**, 4047.
13 R. Sharma, J. H. Baik, C. J. Perera and M. S. Strano, *Nano Lett.*, 2010, **10**, 398.
14 D. E. Jiang, B. G. Sumpter and S. Dai, *J. Phys. Chem. B*, 2006, **110**, 23628.
15 C. Yang and K. N. Houk, *J. Mater. Chem.*, 2011, **21**, 1503.
16 R. C. Haddon, *J. Am. Chem. Soc.*, 1986, **108**, 2837.
17 R. C. Haddon, *J. Am. Chem. Soc.*, 1987, **109**, 1676.
18 R. C. Haddon, *J. Phys. Chem.*, 1987, **91**, 3719.
19 K. D. Ausman, H. W. Rohrs, M. F. Yu and R. S. Ruoff, *Nanotechnology*, 1999, **10**, 258.
20 D. Srivastava, D. W. Brenner, J. D. Schall, K. D. Ausman, M. F. Yu and R. S. Ruoff, *J. Phys. Chem. B*, 1999, **103**, 4330.
21 Y. G. Yanovsky, E. A. Nikitina, Y. N. Karnet and S. M. Nikitin, *Phys. Mesomech.*, 2009, **12**, 254.
22 E. F. Sheka, N. A. Popova, V. A. Popova, E. A. Nikitina and L. H. Shaymardanova, *J. Exp. Theor. Phys.*, 2011, **112**, 602.
23 D. W. Boukhvalov and M. I. Katsnelson, *J. Phys. Chem. C*, 2009, **113**, 14176.
24 R. S. Ruoff, *Nature*, 2012, **483**, 842.
25 X. Y. Fan, R. Nouchi and K. Tanigaki, *J. Phys. Chem. C*, 2011, **115**, 12960.
26 S. Niyogi, E. Bekyarova, M. E. Itkis, H. Zhang, K. Shepperd, J. Hicks, M. Sprinkle, C. Berger, C. N. Lau, W. A. deHeer, E. H. Conrad and R. C. Haddon, *Nano Lett.*, 2010, **10**, 4061.
27 F. M. Koehler, A. Jacobsen, K. Ensslin, C. Stampfer and W. J. Stark, *Small*, 2010, **6**, 1125.
28 E. Bekyarova, M. E. Itkis, P. Ramesh, C. Berger, M. Sprinkle, W. A. de Heer and R. C. Haddon, *J. Am. Chem. Soc.*, 2009, **131**, 1336.
29 A. Sinitskii, A. Dimiev, D. A. Corley, A. A. Fursina, D. V. Kosynkin and J. M. Tour, *ACS Nano*, 2010, **4**, 1949.
30 X. S. Li, Y. W. Zhu, W. W. Cai, M. Borysiak, B. Y. Han, D. Chen, R. D. Piner, L. Colombo and R. S. Ruoff, *Nano Lett.*, 2009, **9**, 4359.
31 Z. H. Ni, T. Yu, Y. H. Lu, Y. Y. Wang, Y. P. Feng and Z. X. Shen, *ACS Nano*, 2008, **2**, 2301.
32 W. Z. Bao, F. Miao, Z. Chen, H. Zhang, W. Y. Jang, C. Dames and C. N. Lau, *Nat. Nanotechnol.*, 2009, **4**, 562.
33 F. Guinea, M. I. Katsnelson and A. K. Geim, *Nat. Phys.*, 2010, **6**, 30.
34 N. Levy, S. A. Burke, K. L. Meaker, M. Panlasigui, A. Zettl, F. Guinea, A. H. Castro Neto and M. F. Crommie, *Science*, 2010, **329**, 544.
35 T. H. Ma, B. Li and T. C. Chang, *Appl. Phys. Lett.*, 2011, **99**, 201901.
36 A. Studer and M. Bossart, *Tetrahedron*, 2001, **57**, 9649–9667.